J Mater Sci (2008) 43:1520–1524
DOI 10.1007/s10853-007-2365-4

Thermoelectric properties of perovskite oxides $La_{1-x}Sr_xCoO_3$ prepared by polymerlized complex method

A. J. Zhou · T. J. Zhu · X. B. Zhao

Received: 18 July 2007 / Accepted: 30 November 2007 / Published online: 1 January 2008

Abstract P-type perovskite oxides $La_{1-x}Sr_xCoO_3$ ($0 \leq x \leq 0.2$) have been prepared using a polymerlized complex method and sintering. The Seebeck coefficient, electrical conductivity, and thermal conductivity of the oxides were studied from room temperature to 773 K. The $\ln(\sigma T)-1/T$ relationships revealed small-polaron hopping mechanism for the higher Sr contents. Large Seebeck coefficients were observed in lightly Sr-doped samples. Sr doping greatly reduced the Seebeck coefficient and enhanced the electrical and thermal conductivity of the samples. The temperature-induced spin-state transition of Co^{3+} ions strongly influenced the transport properties. The highest *ZT* value found in this series of oxides was 0.046 at 300 K for $x = 0.1$.

Introduction

Thermoelectric (TE) effects are based on the transport of heat phonons and charge carriers in a solid. They allow for converting thermal energy directly into electricity and vice versa. The efficiency of a TE material at a given temperature *T* is determined by the dimensionless figure of merit $ZT = \alpha^2\sigma T/\kappa$, where α, σ, and κ are the Seebeck coefficient, electrical conductivity, and thermal conductivity, respectively [1, 2]. Thus, a promising TE material requires a large α and σ, and a low κ to obtain a high figure of merit. Intermetallic compounds or alloys, such as $(Bi, Sb)_2(Te, Se)_3$ [3], filled skutterudites [4], and Si–Ge alloys [5], have high *ZT* values close to unity. However, they are easily decomposed or oxidized at high temperatures under an oxidizing atmosphere. Comparatively, TE oxides have several attractive advantages such as high thermal and chemical stability, excellent oxidation resistance, low costs, and weak toxicity [6], which are of great importance from the point of view of practical applications. Since a large Seebeck coefficient was found in layered oxide $NaCo_2O_4$ exhibiting a promising TE performance [7], some other TE oxides, such as Co-based series of layered structure oxides $Ca_3Co_4O_9$ [8–10], have been reported.

As one of the most interesting perovskite-type oxides, $La_{1-x}Sr_xCoO_3$ has been widely investigated for its potential applications in solid oxide fuel cells [11], nonvolatile memories [12], oxygen permeation membranes [13], and so on. A large Seebeck coefficient was also found in lightly Sr-doped $La_{1-x}Sr_xCoO_3$ with good electronic and ionic conductivities [14, 15], implying the possibility of $La_{1-x}Sr_xCoO_3$ as good candidates for TE applications. A recent study on polycrystalline $La_{0.95}Sr_{0.05}CoO_3$ at low temperatures showed a promising room-temperature *ZT* value of 0.18 [6]. Berggold et al. [16] studied the thermal conductivity and Seebeck coefficient of floating-zone grown $La_{1-x}Sr_xCoO_3$ single crystals below 300 K, and obtained a maximum *ZT* of 0.035 around 225 K for $x = 0.125$. To our knowledge, however, high-temperature thermal conductivity of this series of oxides with different Sr contents was rarely reported.

We have studied the thermoelectric properties above room temperature of perovskite oxide $La_{1-x}Sr_xCoO_3$ ($x = 0$, 0.1) prepared by solid-state reactions [17]. In this work, we presented the electrical and thermal properties of polycrystalline $La_{1-x}Sr_xCoO_3$ ($0 \leq x \leq 0.2$) prepared by

A. J. Zhou · T. J. Zhu · X. B. Zhao (✉)
State Key Laboratory of Silicon Materials, Department of Materials Science and Engineering, Zhejiang University, Hangzhou 310027, China
e-mail: zhaoxb@zju.edu.cn

polymerlized complex method and their dependences on Sr content in the temperature range from 300 to 773 K. The TE potential of the oxides was evaluated based on the present results.

Experimental

$La_{1-x}Sr_xCoO_3$ ($0 \leq x \leq 0.2$) powders were prepared by a polymerlized complex method. Stoichiometric ratio of high-purity metal nitrates $La(NO_3)_3{\cdot}6H_2O$, $Co(NO_3)_3{\cdot}6H_2O$ and $Sr(NO_3)_2$ (99.99%, J&K chemicals) was dissolved in de-ionized water, followed by an addition of 5% polyvinyl alcohol (PVA) solution. The mixture was dehydrated by evaporation below its boiling point with continuous stirring. After the solution became a viscous and homogeneous gel, it was heated up to 423 K to decompose nitrates and remove the carbohydrates. The obtained powder precursor was then calcined at 923 K for 6 h in the flowing oxygen. The resulting black powders were ground, pressed into pellets under 400 MPa, and sintered at 1,273 K for 6 h in oxygen.

The phase structures of the sintered samples were investigated by X-ray diffraction (XRD) using a Rigaku D/MAX-2550P diffractometer with Cu Kα radiation ($\lambda = 1.5406$ Å). The powder morphology was observed by field emission scanning electron microscopy (FESEM) on a FEI-Siron microscope. The measurements for Seebeck coefficient and electrical conductivity were conducted simultaneously in a computer-assisted device in air. For the Seebeck coefficient measurement, a temperature difference of about 4 K between both ends of the sample was generated by an auxiliary heater. The electrical conductivity was measured by a conventional four-probe method. The thermal conductivity κ calculated by $\kappa = a\rho c_p$, where ρ is the sample density measured by Archimedes method, a and c_p, the thermal diffusivity and specific heat of the sample were measured on a Netzsch LFA427 laser flash apparatus and a DSC404 thermal analyser, respectively.

Results and discussion

Figure 1 shows the XRD patterns of the sintered $La_{1-x}Sr_xCoO_3$ ($0 \leq x \leq 0.2$) samples. The diffraction peaks can be definitely indexed to those of the rhombohedral structures with the $R\bar{3}c$ space group, referring to the standard diffraction data JCPDS 48-0123. Slight peak shifts to lower 2θ angles with increasing x value could be observed. The lattice parameters a, c and the axial ratio c/a of the samples calculated from the XRD data are listed in Table 1. Considering the effective ionic radius of Sr^{2+} and La^{3+} for the coordination number of 6 is 1.16 and 1.06 Å [18], respectively, the increasing c/a ratio with increasing x value indicates the successful substitution of Sr for La.

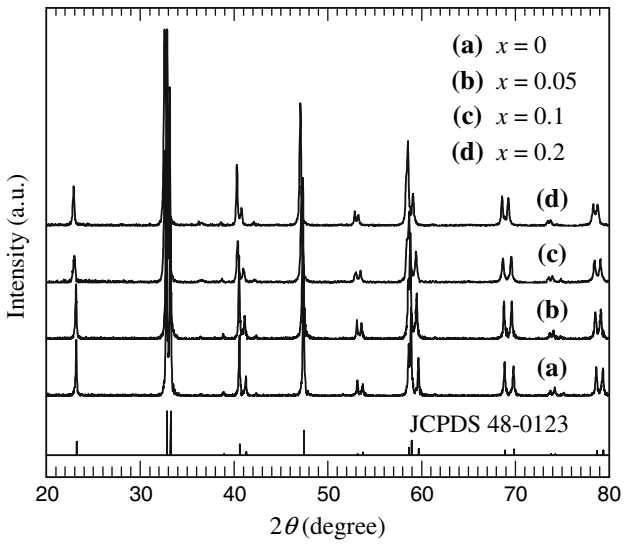

Fig. 1 XRD patterns of the sintered $La_{1-x}Sr_xCoO_3$ ($0 \leq x \leq 0.2$)

Table 1 Lattice parameters a, c and c/a ratio of $La_{1-x}Sr_xCoO_3$ calculated from the XRD patterns and the measured density D of the as-sintered samples

x	0	0.05	0.1	0.2
a (Å)	5.4544	5.4390	5.4284	5.4144
c (Å)	13.108	13.117	13.126	13.136
c/a	2.4033	2.4118	2.4180	2.4262
D (g/cm)	6.99	6.94	6.81	6.50

Figure 2 gives the typical SEM images of the chemically synthesized powder and the sintered sample of $La_{1-x}Sr_xCoO_3$ with $x = 0.1$. It can be seen that the powder is composed of nano-particles of around 50 nm in diameter, while the sintered sample consists of polyhedral grains of around 1 μm in dimension, revealing the obvious grain growth during the sintering. Both the microstructures show homogeneous size distributions. The sintered oxides were dense, seen from the SEM image, and the measured density (listed in Table 1) decreases with increasing Sr content. For all the samples, the relative densities were calculated to be about 95%.

The plots of $\ln(\sigma T)$ versus $1/T$ of the samples in the range of 300–773 K are shown in Fig. 3. The electrical conductivity of all the samples increases with increasing temperature over the measured temperature range, indicating semiconducting behaviour. It seems that the small-polaron hopping mechanism predominates in the lower temperature range with increasing Sr content because the $\ln(\sigma T)$–$1/T$ curves of the samples with $x = 0.1$ and 0.2 show nearly linear relationships at low temperatures, which is in agreement with the previously reported studies [19, 20].

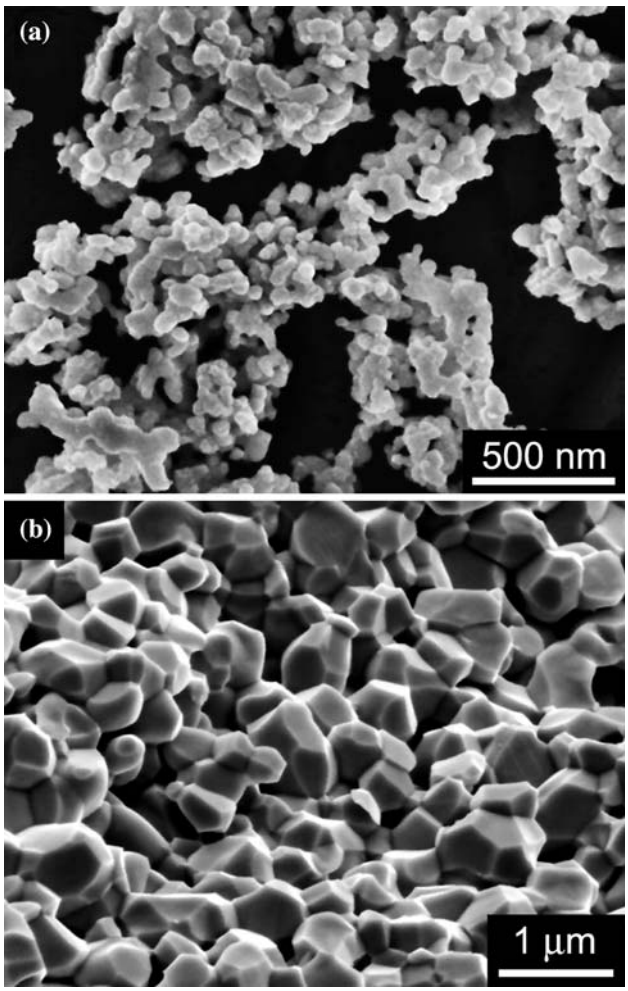

Fig. 2 SEM images of the synthesized powders (**a**) and sintered sample (**b**) with $x = 0.1$

The electrical conductivity of the samples increases with increasing Sr content, which could be attributed to the increase of the carrier concentration by Sr-substitution. The replacement of La^{3+} by Sr^{2+} will create excess negative charges in the lattice, which are compensated either by creation of holes, that is, oxidation of Co^{3+} to Co^{4+}, or by creation of oxygen vacancies to keep the electroneutrality condition [21]. In this study, the holes due to the oxidation of Co^{3+} to Co^{4+} should be responsible for the electrical conductivity behaviour.

The temperature dependence of Seebeck coefficient α of the samples is presented in Fig. 4. The Seebeck coefficients are positive in the measured temperature range, indicating the p-type conduction. The Seebeck coefficients of $La_{1-x}Sr_xCoO_3$ ($0 \leq x \leq 0.2$) exhibit the reverse temperature dependences and imply the change in electrical transport mechanism induced by either Sr doping or temperature increase. In the lower temperature range below about 550 K, the α drops down dramatically with increasing temperature as well as increasing Sr content. However it is nearly independent of temperature in the higher temperature range above 550 K. This notable behaviour is believed to be related to the spin-state transition of Co. Co in $LaCoO_3$ undergoes a gradual spin-state transition from the low-spin (LS) to the intermediate-spin (IS) configuration, and then to the lifting of the local-spin degeneracy (LSD) as temperature increases [14, 19], The spin-state transition mainly contributes to the remarkable decrease of the Seebeck coefficient with increasing temperature below 550 K. Upon Sr substitution, the spin-state transition is suppressed and a number of holes are introduced in $La_{1-x}Sr_xCoO_3$ ($0 \leq x \leq 0.2$), resulting in a dramatic decrease of α with increasing Sr content.

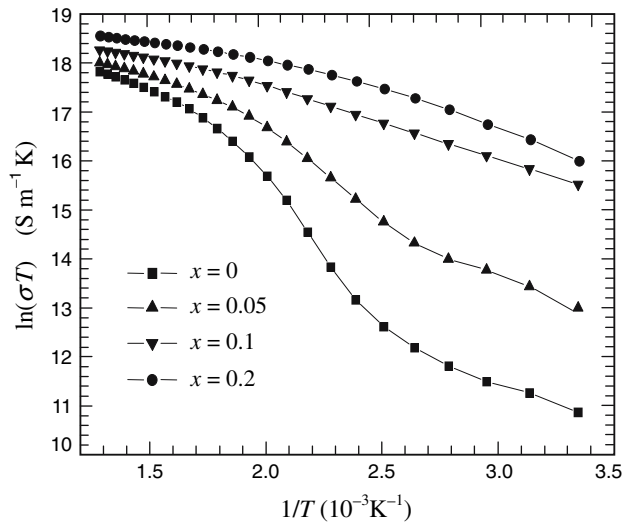

Fig. 3 Plots of $\ln(\sigma T)$ versus $1/T$ for the as-sintered $La_{1-x}Sr_xCoO_3$ samples

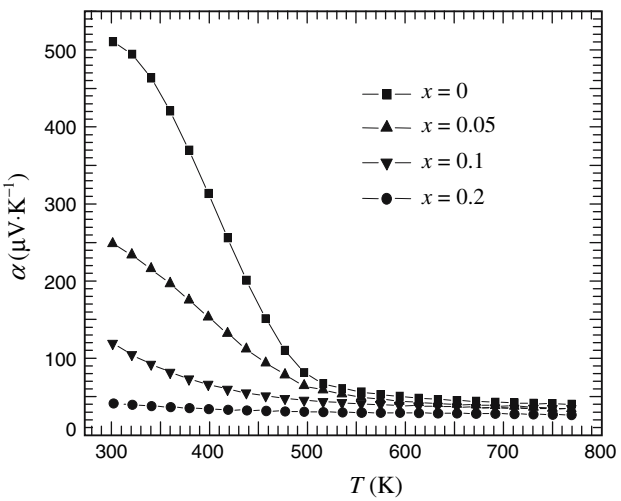

Fig. 4 Temperature dependence of the Seebeck coefficient α of $La_{1-x}Sr_xCoO_3$ ($0 \leq x \leq 0.2$)

At higher temperatures, the Seebeck coefficients show a much less pronounced decreasing rate with increasing temperature because the spin-state transition of Co finishes and the holes contribute a dominating transport term to the Seebeck coefficient. In high enough temperatures, the Seebeck coefficient of doped cobaltates can be determined by the so-called Heikes formula [22]: $\alpha = -(k_B/e)\ln((g_3/g_4)(n/(1-n)))$ where g_3 and g_4 are the number of possible configurations of Co^{3+} and Co^{4+} ions, respectively, and n denotes the content of Co^{4+} ions. At high temperatures, the holes produced due to the thermally activated low-spin Co^{4+} from low-spin Co^{3+} are saturated and hence the α tends to be independent of temperature for all the samples of $La_{1-x}Sr_xCoO_3$ ($0 \le x \le 0.2$), which accords well with the present result.

The low-temperature thermal conductivity of $La_{1-x}Sr_xCoO_3$ has been investigated. It has been observed that both the spin-state transition and Sr-induced disorder may intrinsically suppress the thermal conductivity below 100 K [16]. Figure 5 shows the temperature dependence of thermal conductivity of $La_{1-x}Sr_xCoO_3$ ($0 \le x \le 0.2$) in the temperature range from 300 to 773 K. It can be seen that the thermal conductivity κ increases with Sr content, which is partially attributed to the increase in the holes of Sr-substituted samples. The total thermal conductivity κ of a solid consists of the phonon contribution κ_{ph} and the carrier contribution κ_e which is related to the electrical conductivity σ with $\kappa_e = L_0\sigma T$, where L_0 is the Lorenz number, approximately 1.5×10^{-8} V^2 K^{-2} for non-degenerate semiconductors [23]. The phonon contribution κ_{ph} can be obtained by subtracting κ_e from κ. The κ of all the samples shows an increasing trend as the temperature increases, which contributes to the dramatic increase of the carrier thermal conductivity with increasing temperature. The phonon contribution is the dominating part of the κ for $La_{1-x}Sr_xCoO_3$ ($0 \le x \le 0.2$). As the temperature goes up, although the electrical part κ_e is greatly enhanced due to the enhanced electrical conductivity, the κ_{ph} still remains to be 65–80% of κ, suggesting that it is possible to increase the figure of merit ZT, if the phonon thermal conductivity can be effectively reduced by optimizing compositions and microstructure to enhance phonon scattering. Also note that phonon thermal conductivity takes a maximum of around 400–700 K, which is possibly related to the "Umklapp-process" of phonon–phonon interactions or the enhanced electron–phonon coupling. However, more detailed investigation is needed to clarify the supposition.

The calculated dimensionless figure of merit ZT as a function of temperature is shown in Fig. 6. The highest value of $ZT_{max} = 0.046$ was obtained in the sample with $x = 0.1$ at room temperature. This value is higher than those of the samples prepared by solid-state reaction [17], because the latter has lower electrical conductivity. The present value is also comparable to that reported by Berggold et al. [16] ($ZT_{max} = 0.035$) and Zhang et al. [20] ($ZT_{max} = 0.033$), but lower than that reported by Androulakis et al. [6] for $La_{0.95}Sr_{0.05}CoO_3$ ($ZT_{max} = 0.18$ at 300 K) mainly due to the unusually large Seebeck coefficient in their report. It can be seen from the present results that the high-temperature TE performance of $La_{1-x}Sr_xCoO_3$ is not as promising as expected, because the α, σ, and κ do not simultaneously exhibit a favourable variation with increasing temperature. However, the order of magnitude of the present ZT_{max} value is comparable to that of the $NaCo_2O_4$ with a ZT_{max} value of 0.03 at room temperature [24], which demonstrates that the cobalt-based perovskite oxide can be one of the potential candidates for TE materials. For possible TE applications

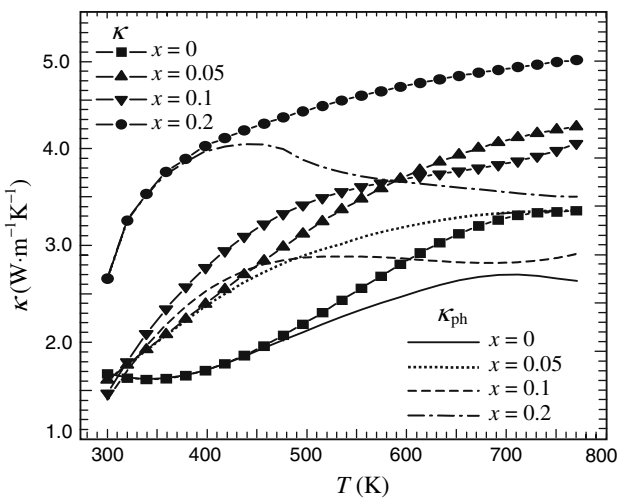

Fig. 5 Temperature dependences of thermal conductivity κ and the phonon contribution κ_{ph} of the $La_{1-x}Sr_xCoO_3$ samples

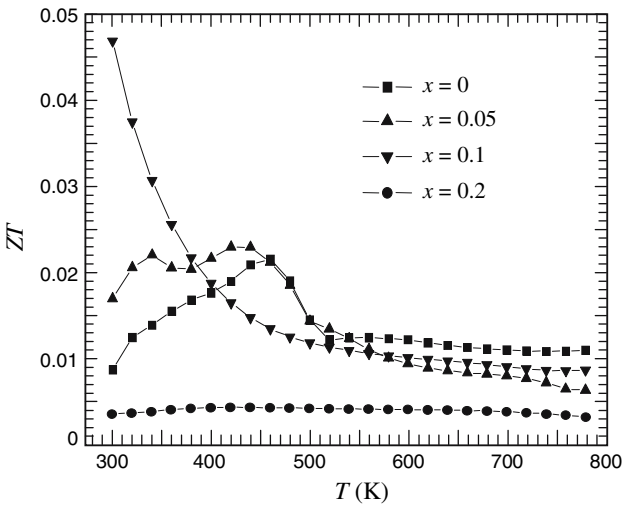

Fig. 6 The dimensionless figures of merit ZT of $La_{1-x}Sr_xCoO_3$ ($0 \le x \le 0.2$) as a function of temperature

of these oxides, some compositional or processing optimizations are needed to achieve higher figures of merit.

Conclusions

Polycrystalline samples of p-type perovskite $La_{1-x}Sr_xCoO_3$ ($0 \leq x \leq 0.2$) have been prepared using polymerlized complex method, followed by high-temperature sintering. The thermoelectric properties were investigated from room temperature to 773 K. The particle size of the chemically synthesized powders was around 50 nm, while for the sintered samples the grain size grew up to be in micrometers. Sr doping increases the electrical and thermal conductivity, and small polaron conduction mechanism predominates with increasing Sr content. The Seebeck coefficient remarkably decreases with increasing Sr content and temperature due to the change of Co ions in the oxides. The spin-state transition of Co intrinsically influences the transport behaviours. The phonon contribution of the thermal conductivity of all the samples is dominant over the measured temperature range. The highest *ZT* values obtained for these oxides are of order of 0.04, which is comparable to those of the TE oxide $NaCo_2O_4$.

Acknowledgements The authors would like to thank Dr. E. Müller, Dr. C. Stiewe, and W. Schönau from Institute of Materials Research, German Aerospace Center (DLR), for the measurements of thermal properties. TJZ would like to thank Dr. Jian He from Department of Physics and Astronomy, Clemson University, USA, for the discussion and comments. This work was supported by the National Science Foundation of China (50471039, 50522203) and PFDP of the Education Ministry of China (20060335126).

References

1. DiSalvo FJ (1999) Science 285:703
2. Sales BC (2002) Science 295:1248
3. Yamashita O, Tomiyoshi S, Makita K (2003) J Appl Phys 93:368
4. Sales BC, Mandrus D, Williams RK (1996) Science 272:1325
5. Koga T, Cronin SB, Dresselhaus MS, Liu JL, Wang KL (2000) Appl Phys Lett 77:1490
6. Androulakis J, Migiakis P, Giapintzakis J (2004) Appl Phys Lett 84:1099
7. Terasaki I, Sasago Y, Uchinokura K (1997) Phys Rev B 56:12685
8. Prevel M, Lemonnier S, Klein Y, Hebert S, Chateigner D, Ouladdiaf B, Noudem JG (2005) J Appl Phys 98:093706
9. Hu YF, Sutter E, Si WD, Li Q (2005) Appl Phys Lett 87:171912
10. Liu YH, Lin YH, Shi Z, Nan CW, Shen ZJ (2005) J Am Ceram Soc 88:1337
11. Inagaki T, Miura K, Yoshida H, Maric R, Ohara S, Zhang X, Mukai K, Fukui T (2000) J Power Sources 86:347
12. Wang F, Leppavuori S (1997) J Appl Phys 82:1293
13. Chen CH, Bouwmeester HJM, van Doorn RHE, Kruidhof H, Burggraaf AJ (1997) Solid State Ionics 98:7
14. Senarís-Rodríguez MA, Goodenough JB (1995) J Solid State Chem 118:323
15. Teraoka Y, Zhang HM, Okamoto K, Yamazoe N (1988) Mater Res Bull 23:51
16. Berggold K, Kriener M, Zobel C, Reichl A, Reuther M, Muller R, Freimuth A, Lorenz T (2005) Phys Rev B 72:155116
17. Zhou AJ, Zhu TJ, Zhao XB (2006) Mater Sci Eng B 128:174
18. Shannon RD, Prewitt CT (1969) Acta Cryst B25:925
19. Senarís-Rodríguez MA, Goodenough JB (1995) J Solid State Chem 116:224
20. Zhang X, Li XM, Chen TL, Chen LD (2006) J Cryst Growth 286:1
21. Mineshige A, Kobune M, Fujii S, Ogumi Z, Inaba M, Yao T, Kikuchi K (1999) J Solid State Chem 142:374
22. Koshibae W, Tsutsui K, Maekawa S (2000) Phys Rev B 62:6869
23. Venkatasubramanian R, Siivola E, Colpitts T, O'Quinn B (2001) Nature 413:597
24. Takahata K, Iguchi Y, Tanaka D, Itoh T, Terasaki I (2000) Phys Rev B 61:12551